

Cyclic Event Identification and Fatigue Damage Assessment for Multiaxial Mission Loadings

Mr. Eric Goodin¹, Dr. Alan Kallmeyer¹, and Dr. Peter Kurath²

¹ Department of Mechanical Engineering, North Dakota State University, Fargo, ND

² Department of Mechanical Engineering, University of Illinois, Urbana, IL

ABSTRACT

Several multiaxial (tension/torsion) mission-history tests were conducted on smooth bars of Ti-6Al-4V. The mission histories were constructed of a single out-of-phase LCF cycle (in the form of a “box” or “check” path) coupled with 5 to 50 small HCF cycles. The stress paths and magnitudes for the LCF and HCF cycles were chosen to produce significantly different damage levels on different planes, as predicted by critical plane models that have been found to provide good agreement with constant amplitude fatigue data. Using Miner’s algorithm for damage summation and traditional event identification, the HCF cycles should have had a negligible effect on the LCF mission lives. However, the experimental results illustrated widely differing effects. In this paper, alternative techniques are discussed which relate to the identification of cyclic events, the calculation of fatigue damage resulting from an event, and the accumulation of damage which takes into account the nonlinear behavior resulting from LCF/HCF interactions. A nonlinear damage summation method based on the Damage Curve Approach was found to provide excellent agreement with the experimental results when applied in conjunction with the Findley critical plane model.

INTRODUCTION

The interaction between LCF (high damage) and HCF (low damage) cycles in a variable load history, or “mission” history, is an area of concern when developing fatigue damage assessment methods for turbine engine materials. The consideration of such interaction effects within multiaxial loadings gives rise to some additional challenges. For example, the definition of a cyclic event can be ambiguous when different components of the stress tensor are cycling out-of-phase of one another. Furthermore, the use of a “critical-plane” model for damage assessment can add additional complications when different events in the history cause maximum damage on different planes. Past research [1] has demonstrated that damage summation methods based on existing multiaxial fatigue damage parameters and linear damage accumulation are often highly non-conservative, indicating an interaction effect between LCF and HCF cycles. These effects are more pronounced when out of phase loading comprises one of the cyclic events. Similar LCF/HCF interaction effects have been observed under uniaxial loading conditions. A variety of techniques have been proposed to accommodate experimental observations, including non-linear damage rules, modification of the baseline damage curve, and extended interpretation of the damage parameter.

In previous studies [1, 2], the authors have evaluated over 20 multiaxial fatigue damage parameters by comparison to numerous Ti-6Al-4V uniaxial data and approximately thirty biaxial smooth bar tests which encompassed a variety of mean stress conditions and non-proportionality. Both the level of loading and shape of the paths considered in those studies were intended to simplify portions of actual service events. Figure 1 highlights some of the non-proportional load

paths considered in the previous investigations. The reader is referred to reference [2] for other details of the testing and specimen design.

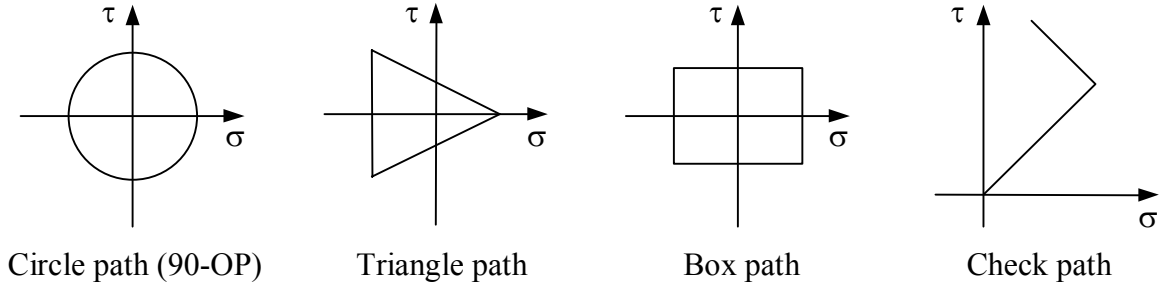


Figure 1. Non-proportional biaxial load paths.

The previous model evaluations considered both “equivalent-stress” based models and “critical-plane” parameters [2]. The advantage of an equivalent stress model is its relative simplicity in implementation; a scalar parameter is used to represent all components in the cyclic stress tensor. However, with certain exceptions, the equivalent stress models were found to provide generally poorer correlation of the biaxial test data, in comparison to the critical plane models. The critical plane approaches require an iterative search algorithm to identify the critical plane, or the plane of expected crack initiation. The more complex implementation has in the past limited their use; however, modern computational resources have somewhat negated this disadvantage.

FINDLEY MODEL

From the earlier analyses [2], the Findley critical plane model was identified as providing the best overall correlation of the biaxial test data with the uniaxial baseline curve. The Findley model [3] characterizes damage on a given plane by addition of the maximum normal stress (multiplied by an adjustable factor, k) and the maximum shear stress amplitude on that plane. The resulting parameter, hereafter called the Findley Parameter (FP), is shown in Eq. (1). In the present study, k is considered to be constant over the life of the material. The plane on which crack initiation is assumed to begin, or critical plane, is then defined as the plane that experiences the maximum value of FP. This model has been shown to reasonably correlate uniaxial and biaxial data for Ti-6Al-4V using a dual-power law relation, as shown in Eq. (1).

$$FP = \frac{\Delta\tau}{2} + k\sigma_n^{\max} = AN^b + CN^d \quad (1)$$

An important consideration in the use of Eq. (1) is the definition of the maximum normal stress, σ_n^{\max} . This equivocal term could take on a variety of definitions. For example, it could be considered to represent the maximum stress experienced over the course of one loading cycle. This interpretation, which predicts the greatest amount of damage, is a logical choice, particularly when the applied loading conditions are in-phase and proportional. However, there exist many occasions where the loadings occur either out-of-phase or non-proportionally, or

both. This gives rise to another definition for the maximum normal stress; that is, the normal stress that occurs at a shear stress reversal point within a cycle. Figure 2 illustrates the difference between the two definitions. As shown, the first definition experiences $\sigma_{\max} = \sigma_C$ and is representative of what is traditionally believed to be the more damaging. The second definition is shown as having a somewhat smaller maximum normal stress, labeled σ_B . Although the normal stress may be smaller, by definition the shear stress is larger at this instant. Presuming crack initiation to be a shear-driven process in many materials, this model may be expected to provide a more accurate representation of the mechanics of crack initiation. Note that if the normal and shear stress histories are applied in-phase then both definitions are identical.

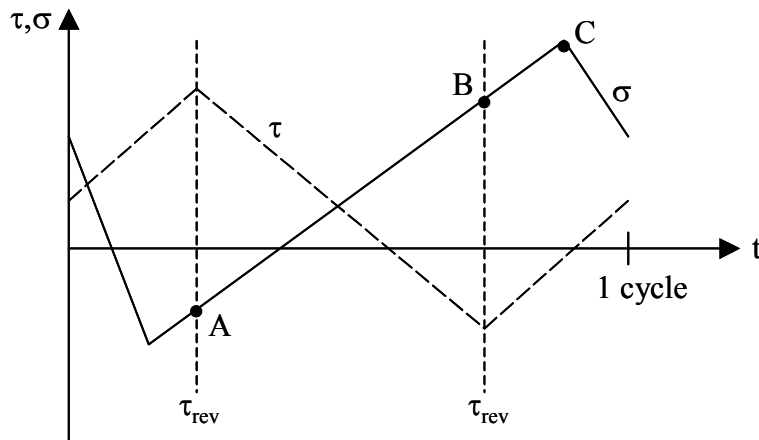


Figure 2. Example biaxial stress history over 1 cycle, showing different methods used to define the normal stress term in the Findley model. The dashed line is the shear stress and the solid line is the normal stress.

Based on the results of earlier investigations [1], the second definition of the maximum normal stress ($\sigma_{\max} = \sigma_B$) was used in the present study. Figure 3 illustrates the Findley model being applied to a set of uniaxial (top) and biaxial (bottom) Ti-6Al-4V data. The curve shown is a “best-fit” curve to the uniaxial data, obtained by minimizing the squared error between the experimental damage calculated using the Findley model and the aforementioned dual-power law prediction equation. This curve serves as a baseline to determine the validity of the model when attempting to predict multiaxial failure. There are two features that need clarification on the uniaxial (top) figure. First, the “step data” located at the higher end of the failure life were not included in the calculation of the best-fit curve. It was noted that these tests appeared to result in slightly higher stress levels at long life than the single-load tests. Second, a “threshold” line is shown on the plot. This line indicates the level of the Findley parameter below which the applied loadings are assumed to have negligible effect on the fatigue life of the specimen. As can be seen from the figure, the prediction curve continues to drop at higher life, even though there is no data to suggest the continued trend above 10^9 cycles. This results in overly conservative life predictions when extrapolating the curve to long-life regions. Examining the calculated Findley parameters and observing that no failure occurred below 34 ksi, a lower bound to failure was established at this level.

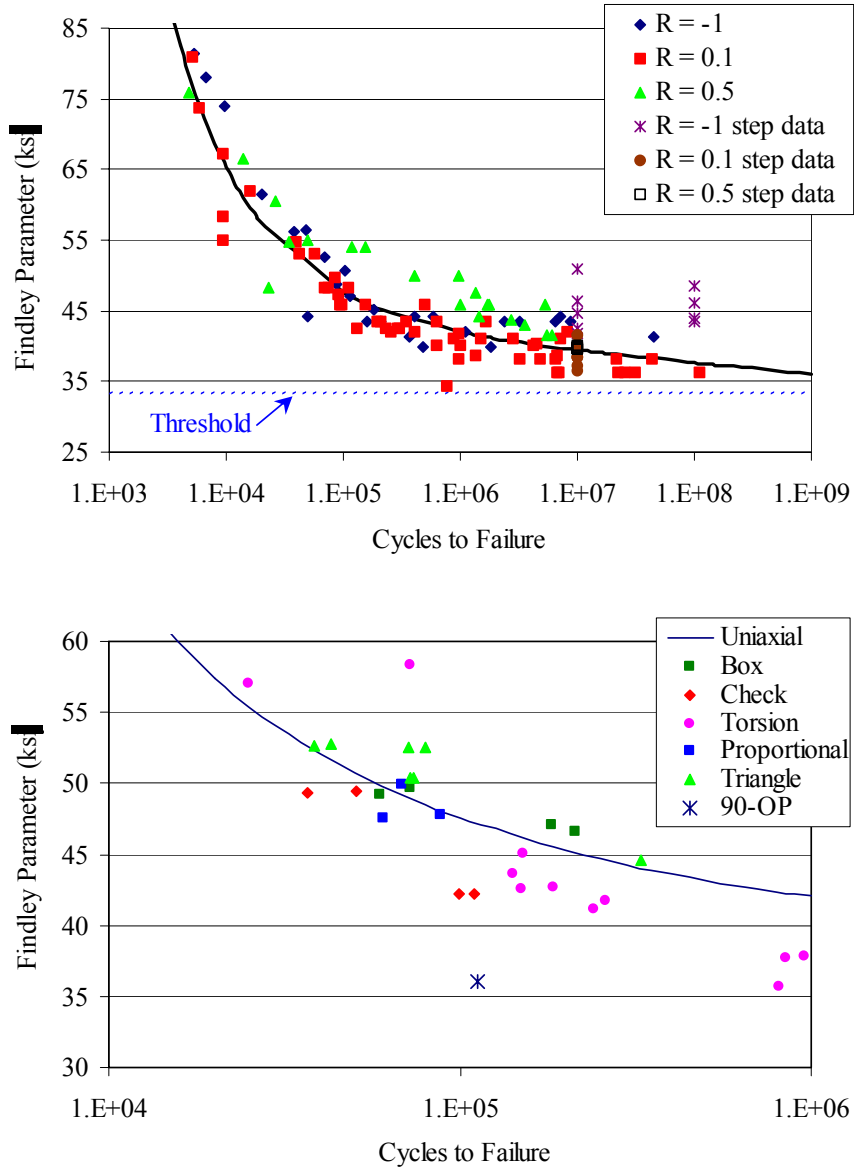


Figure 3. Findley model applied to Ti-6Al-4V uniaxial data (top) and biaxial data (bottom).

The Findley model provides a reasonably good prediction for both the uniaxial and biaxial data. Much of the biaxial data collapses around the prediction curve fairly well, with a few exceptions. It is evident that the life of the circle (90-OP) path is over-predicted, and that all of the check and most of the torsion points were slightly non-conservative. In an attempt to obtain a better curve-fit, the prediction equation was reevaluated by fitting the torsional test data rather than the uniaxial data. The resulting curve, shown in Figure 4, provided a better overall correlation of the biaxial data, although the 90-OP test was still highly non-conservative. However, the fit of the uniaxial data to the torsional curve was very poor, rendering this approach much worse overall in comparison to the previous method (Fig. 3).

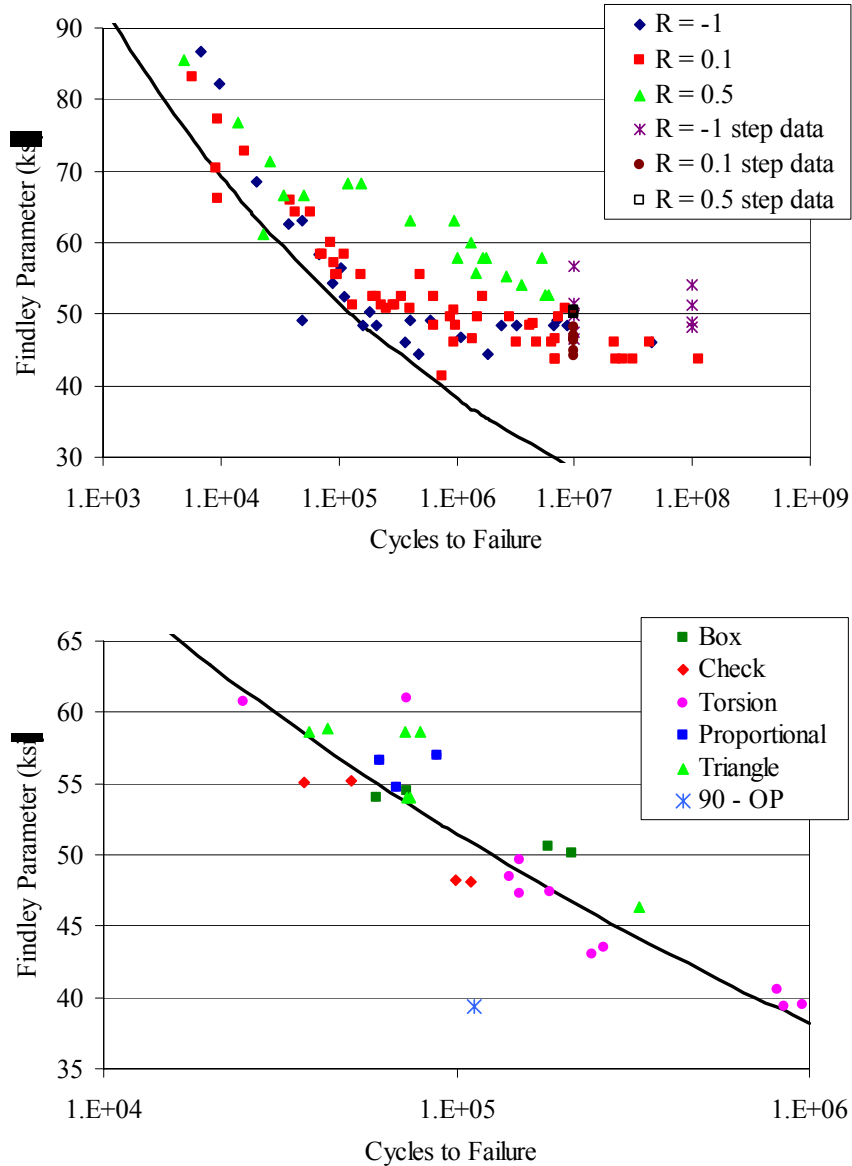


Figure 4. Findley model applied to uniaxial (top) and biaxial (bottom) Ti-6Al-4V data, with curve fit applied to torsional data.

MISSION HISTORIES: RESULTS AND MODEL COMPARISONS

To better understand the ability of the Findley model to predict the potential LCF/HCF interaction effects in a multiaxial, variable load history, several biaxial mission tests were conducted on similar specimens as used in the previous biaxial testing. There were two variations of the mission histories, each designed to represent the effects a component could experience while in service. From these results, the authors could experimentally assess the LCF/HCF interactions, as well as evaluate the effectiveness of cumulative damage models under combined loading conditions. In these histories, a relatively few high-damage (LCF) cycles were applied periodically within a larger number of low-damage (HCF) cycles. The LCF load

path is what gives rise to the mission type. As illustrated in Figure 5, the two mission histories were based on the box path and the check path (LCF cycles). The HCF cycles were defined as small portions of the LCF cycles. The differences between the LCF and HCF cycle shapes and amplitudes generated different critical planes within a loading cycle, as predicted by the Findley model, and provided a differentiation among the fatigue damage produced by each cycle. The stress levels were applied to produce LCF lives in the range of 10^4 to 10^5 cycles, while the HCF stress levels were selected to produce lives on the order of 10^8 to 10^9 cycles, as per the Findley model predictions.

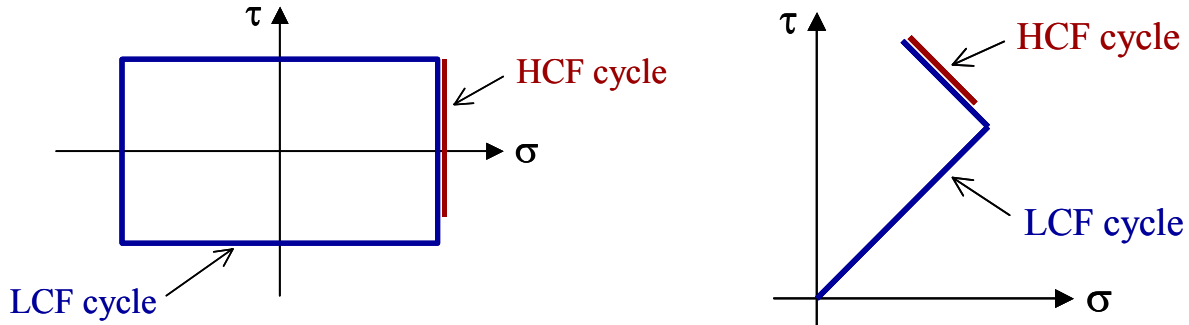


Figure 5. Simulated mission histories, showing LCF and HCF cycles for the box path and the check path.

Three sets of mission history tests were conducted, two based on the box path and one based on the check path. Two samples were run at each load level. Each mission history consisted of one LCF cycle followed by a larger number of HCF cycles. For the two box path histories, one consisted of 50 HCF subcycles (Box 1) and the other consisted of 5 HCF subcycles (Box 2). It should be noted the same subcycle was utilized in both missions. The check path consisted of 50 subcycles in addition to the LCF cycle. These mission histories were repeatedly applied to round bar specimens of Ti-6Al-4V until fracture. The number of cycles completed before failure is defined as the mission life. The reader is referred to [1] for a more thorough discussion of mission history model comparisons.

The experimental results for the mission histories are shown in Table 1, along with the corresponding mission life predictions using the Findley model in conjunction with a linear cumulative damage rule. As is evident from these results, the predicted mission lives were essentially identical to the predicted LCF lives in all cases, when a linear damage assumption was used. This is not surprising, since the HCF lives were predicted to be roughly four orders of magnitude larger than the LCF lives. Thus, utilizing a linear damage rule, a substantial number of HCF cycles would need to be applied before they would begin to influence the mission life.

The experimental data, however, indicate different results. For the two box missions, the HCF cycles substantially influenced the mission lives. Specifically, when 50 HCF cycles were applied (Box 1), the mission lives decreased by a factor of three relative to the LCF lives. When only 5 HCF cycles were applied, the mission lives still decreased by roughly 33%. This indicates a significantly nonlinear damage accumulation rate in the box path. However, in the case of the check path, 50 HCF cycles did not produce any reduction in the mission life, even though they were predicted to cause similar damage levels as the subcycles in the box path. Thus, it is evident that the damage accumulation rate, and the effects of LCF/HCF interactions, is load path dependent.

Table 1
Mission History Results and Model Comparisons
using Findley Parameter with Linear Cumulative Damage Rule

Cycle/Mission	<u>Mission Histories</u>		
	Box 1 1 LCF/50 HCF	Box 2 1 LCF/5 HCF	Check 1 LCF/50 HCF
Experimental LCF Lives	59,432 / 72,360	59,432 / 72,360	50,568 / 36,920
Average	65,900	65,900	43,700
Predicted LCF Life (Plane)	66,900 (122°)	65,500 (122°)	66,900 (12°)
Predicted HCF Life (Plane)	3.0×10^8 (10°)	2.3×10^8 (10°)	1.9×10^8 (48°)
Experimental Mission Life	19,420 / 21,422	48,787 / 39,480	44,544 / 49,776
Average	20,400	44,100	47,200
Predicted Mission Life (Plane)	66,900 (122°)	65,400 (122°)	66,600 (12°)

By consideration of the results in Table 1, it is evident that two factors merit further attention. The first is the effect of load path dependence on the damage accumulation rate; i.e., why are the HCF cycles so much more damaging in the case of the box path than in the check path? The second factor is the damage accumulation rule itself; i.e., can a suitable cumulative damage rule be found which will predict the nonlinear nature of the LCF/HCF interactions?

Load Path Dependence of LCF/HCF Interactions

To address the issue of load path dependence, an evaluation was performed for both the box path and check path to determine which plane experiences the most damage from the combined LCF and HCF cycles, according to the Findley model. As illustrated in Figure 6, the box path exhibits four LCF maxima representing approximately the same damage value. Thus, it is reasonable to expect that there would be an equal probability that a crack may initiate on any of these four planes. When incorporated into a mission history containing LCF and HCF cycles, it would subsequently be expected that the plane of maximum damage potential would be the LCF critical plane experiencing the maximum damage from the HCF subcycles. From Figure 6, it is evident that the LCF critical plane at 12° also nearly coincides with an HCF critical plane; i.e., the LCF and HCF damage curves experience a peak at roughly the same plane orientation.

A similar evaluation was performed with the check mission, shown in Figure 7. In this instance there were only two peaks associated with the LCF parameter. Note, however, that the peak in the HCF curve did not correspond closely to a peak in the LCF curve. Further examination revealed that the maximum HCF Findley parameter on an LCF critical plane was only 32.6 ksi. This value falls below the prescribed threshold of 34 ksi determined earlier. Therefore, the damage associated with the HCF subcycles would be predicted to have a negligible effect on the fatigue life of the specimen.

This distinction of the applied HCF damage on the LCF critical plane validates the experimental evidence showing a load path dependence on the influence of the HCF cycles. In other words, even though both HCF cycles were predicted to cause the same degree of damage on their corresponding critical planes, the fact that the HCF critical plane for the box path coincided with an LCF critical plane caused the box missions to be much more influenced by the

HCF cycles than the check mission, where the LCF and HCF critical planes did not coincide. It should be noted that a multiaxial parameter that does not identify critical plane orientations would not be capable of recognizing the load path dependence of HCF damage observed in this study. This is an important point in regard to equivalent-stress based multiaxial parameters, which do not distinguish critical plane orientations with respect to fatigue damage.

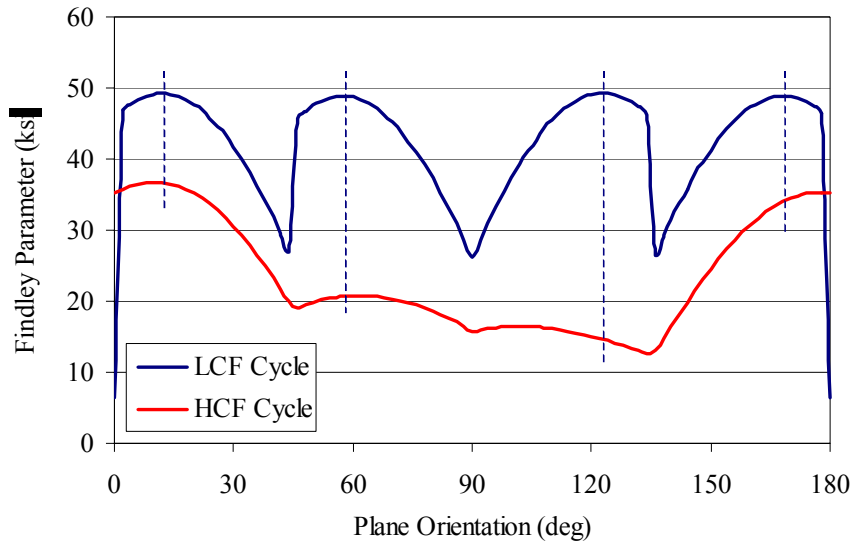


Figure 6. Variation of the Findley Parameter with plane orientation for the box path (LCF and HCF cycles).

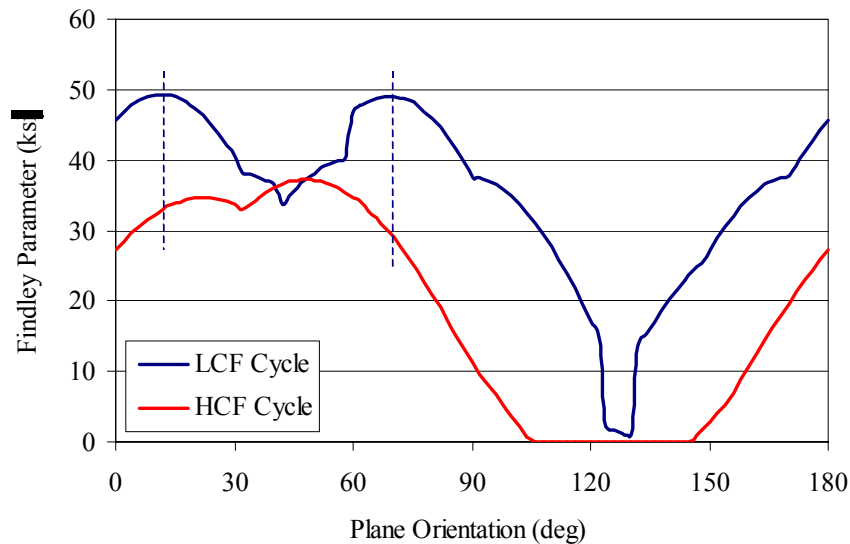


Figure 7. Variation of the Findley Parameter with plane orientation for the check path (LCF and HCF cycles).

Nonlinear Damage Accumulation Rule

The manner in which damage was initially determined for the multiaxial loadings was to sum up all of the LCF and HCF cycles as per the Palmgren-Miner Rule. However, the argument was made that the discrepancy between experimental and predicted mission lives for the box path might be the result of a nonlinear damage accumulation. Recent work [4, 5] has expressed the possibility of two models that possess the likelihood of reducing this difference, the Double Linear Damage Rule (DLDR) and the Damage Curve Approach (DCA). The DLDR proposes to create two separate linear damage relations; one for Phase I and one for Phase II crack growth. The difficulty in utilizing this model is the failure to distinguish between crack initiation and crack propagation. The authors, therefore, elected to implement the DCA model. This model makes use of relative damage and employs the concept of remaining life for a specimen. The DCA approach can be seen in its general form in Eq. (2), where n is the number of applied cycles, N_f is the number of cycles to failure, N_{ref} is the life level at which damage accumulates linearly, and α is a material parameter. Since the point at which damage accumulates in a linear manner is an unknown, N_{ref} can be taken as 1, which has the added effect of simplifying the general equation [5].

$$D = \left(\frac{n}{N_f} \right) \left(\frac{N_f}{N_{ref}} \right)^\alpha \quad (2)$$

The following form of the DCA equation, Eq. (3), describes a two-level loading condition in which one cycle experiences a stress of a given magnitude followed by another cycle(s) of different (either larger or smaller) stress magnitude. As can be seen, this expression predicts greater nonlinearity in damage accumulation as the difference between N_1 and N_2 increases. In this equation, n_1 and n_2 are the number of applied cycles for one mission. N_1 and N_2 are the number of cycles to failure corresponding to the first and second loading blocks (in our case the number of LCF and HCF cycles), respectively. Again, α is a material property that needs to be determined. According to McGaw [5], α is generally taken to be 0.4 based on two-level load testing of steels and titanium alloys. However, analysis of the DCA approach in this study yielded an α of 0.72 when applied to the box and check missions.

$$\frac{n_2}{N_2} = 1 - \left(\frac{n_1}{N_1} \right) \left(\frac{N_1}{N_2} \right)^\alpha \quad (3)$$

Figure 8(a) illustrates the general DCA model. Notice that damage develops earlier and at a faster rate when N is smaller, which is indicative of an LCF loading block. Also shown is the DCA for a two-level loading history, Fig. 8(b). As the difference between N_1 and N_2 decreases the damage accumulation becomes more linear until, when N_1 equals N_2 , the DCA reduces to the Palmgren-Miner Rule.

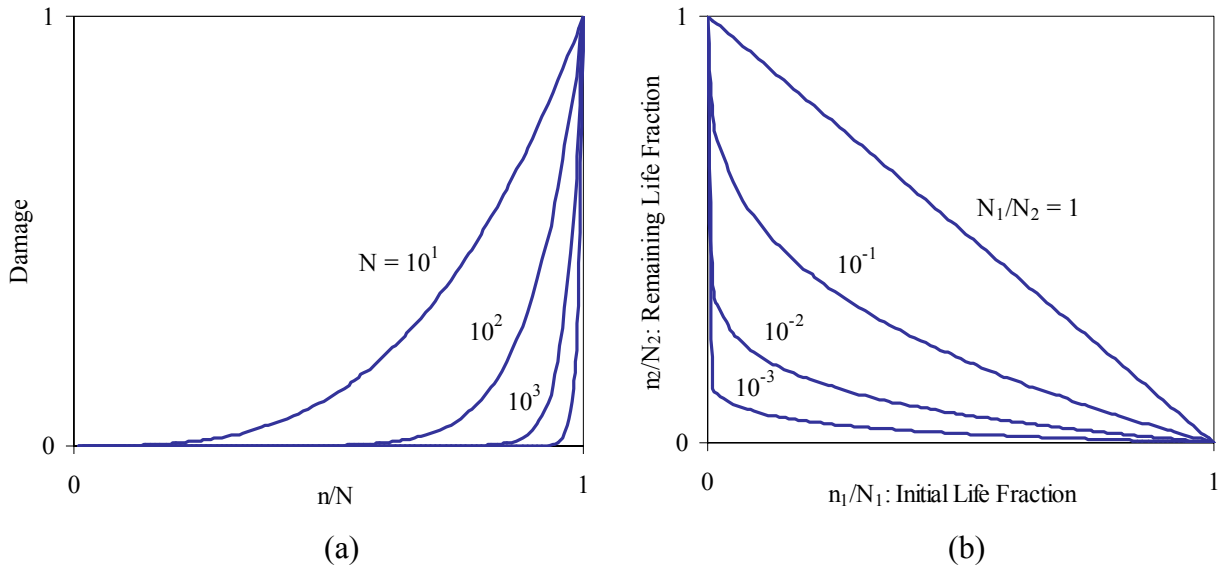


Figure 8. Graphical interpretation of the DCA model.

An important feature of the DCA model is the manner in which the loads are applied. McGaw [5] evaluated the effects on damage for both a two-level single-block loading and a two-level multi-block loading (Figure 9). The result indicated the multi-block loading experienced nonlinear damage accumulation to a greater degree. The reader will recall that the testing conditions for the box and check path mission histories consisted of this two-level multi-block loading. Therefore, these histories would be expected to exhibit significant nonlinear damage accumulation.

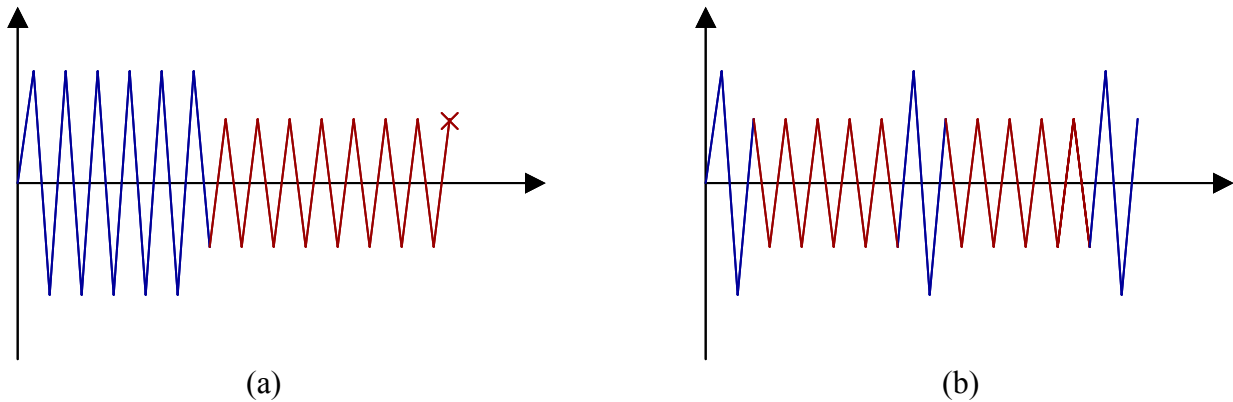


Figure 9. Loading patterns: (a) two-level single-block loading and (b) two-level multi-block loading.

The results of the mission-history life predictions, using the Findley model with the threshold stress level in conjunction with the DCA model, are shown in Table 2 along with the experimental results. As previously noted, a value of $\alpha = 0.72$ was found to provide the best correlation with experimental results. It can be seen that the predicted mission lives for the two box histories are in excellent agreement with the experimental lives using the DCA model.

In the case of the check mission, since the HCF Findley parameter on the LCF critical plane was less than the threshold value, the HCF life on that plane was taken as infinite. Thus, the DCA model predicted no effect of the HCF cycles on the check mission life. Although the predicted and experimental mission lives for the check history were not in as good agreement as for the box history, the discrepancy was due to the LCF life prediction, not due to the failure of the nonlinear damage model. Nevertheless, it should be noted that all the life predictions using the Findley model and Damage Curve Approach are within reasonable bounds.

Table 2
Mission History Results and Model Comparisons
using Findley Parameter with Nonlinear Cumulative Damage Rule (DCA)

Cycle/Mission	<u>Mission Histories</u>		
	Box 1 1 LCF/50 HCF	Box 2 1 LCF/5 HCF	Check 1 LCF/50 HCF
Experimental LCF Lives	59,432 / 72,360	59,432 / 72,360	50,568 / 36,920
Average	65,900	65,900	43,700
Predicted LCF Life (Plane)	66,900 (12°)	65,500 (12°)	66,900 (12°)
Predicted HCF Life on LCF Plane	3.0×10^8	2.3×10^8	∞
Experimental Mission Life	19,420 / 21,422	48,787 / 39,480	44,544 / 49,776
Average	20,400	44,100	47,200
Predicted Mission Life (Plane)	18,260 (12°)	45,880 (12°)	66,900 (12°)

SUMMARY AND CONCLUSIONS

Comparatively small amplitude subcycles (HCF cycles) have a much greater effect on the fatigue life of Ti-6Al-4V than predicted by linear damage accumulation, such as that posed by the Palmgren-Miner Rule. However, the degree of the subcycle influence is highly dependent on the applied load path. This is evidenced from the evaluation of box and check path mission histories containing LCF and HCF cycles. It is necessary to consider the relationship between the LCF and HCF critical planes to account for this dependence. As a result, a multiaxial parameter, such as an equivalent-stress parameter, that cannot distinguish between the critical plane orientations of LCF and HCF cycles may not adequately predict this load path dependence.

The Damage Curve Approach (DCA) better describes the nonlinearity of damage accumulation in these more complicated loading patterns. This method has been shown to provide accurate mission life predictions for two-step (LCF/HCF) loadings. The material property, α , in this model must be experimentally determined from variable loading tests. This value has been determined to be approximately 0.72 for Ti-6Al-4V, which is higher than the previously reported value of 0.4 for various titanium alloys.

It is noted that only two-level (LCF/HCF) block loadings were considered in this study. A more thorough evaluation should be performed to determine the validity of the DCA in predicting the fatigue lives of more complex loading histories.

ACKNOWLEDGEMENT

This work was partially supported under Air Force Contract No. F49620-99-C-0007. The contract is being administrated through the University of Dayton Research Institute under subcontracts RSC99013 with North Dakota Sate University and RSC98007 with the University of Illinois.

REFERENCES

1. Goodin, E., Kallmeyer, A. R., and Kurath, P., "Multiaxial Fatigue Evaluation of Ti-6Al-4V under Simulated Mission Histories," Proceedings of the 7th National Turbine Engine High Cycle Fatigue Conference, West Palm Beach, FL, 2002.
2. Krgo, A., Kallmeyer, A. R., and Kurath, P., "Evaluation of HCF Multiaxial Fatigue Life Prediction Methodologies for Ti-6Al-4V," Proceedings of the 5th National Turbine Engine High Cycle Fatigue Conference, Arizona, 2000.
3. Findley, W. N., "Fatigue of Metals Under Combinations of Stresses," *Transactions*, ASME, Vol. 79, 1957, pp. 1337-1348.
4. Manson, S. S., and Halford, G. R., "Practical Implementation of the Double Linear Damage Rule and Damage Curve Approach for Treating Cumulative Fatigue Damage," *Int. J. of Fracture*, Vol. 17, 1981, pp. 169-192.
5. McGaw, M. A., "Approaches to Cumulative Damage Analysis," *Material Durability/Life Prediction Modeling: Materials for the 21st Century*, ASME PVP-Vol. 290, 1994, pp. 95-106.